14th International Particle Accelerator Conference,Venice, Italy JACoW Publishing
ISBN: 978-3-95450-231-8 ISSN: 2673-5490 doi: 10.18429/JACoW-IPAC2023-WEPL075

MODELING FOR THE PHASED INJECTOR UPGRADE FOR 12 GeV CEBAF*

A. Hofler†, R. Kazimi, Y. Wang, K. Surles-Law
Thomas Jefferson National Accelerator Facility, Newport News, VA, USA

Abstract

As a follow on to the 12 GeV upgrade to the Continuous Electron Beam Accelerator Facility, the front end of the DC photo-gun-based injector has gone through a phased upgrade. The first phase focused on the beamline between the gun and the RF chopper system, and the second phase addresses the beamline after the RF chopper system including replacing the capture section and quarter cryomodule with a new booster module containing a 2-cell and 7-cell cavity string. Throughout the design process, we maintained and developed three models, one for the existing injector and one for each of the upgrade phases. With these models, we evaluated proposed hardware upgrades, evaluated and determined optimized beamline element positions, developed buncher voltage requirements, and established settings for optimal injector running. Here, we describe the models and provide brief summaries of the studies and Phase 1 commissioning.

INJECTOR UPGRADE PATH OVERVIEW

Prior to the injector upgrade for the 12 GeV Continuous Electron Beam Accelerator Facility (CEBAF), the injector layout for 6 GeV CEBAF (Fig. 1a) [1, 2] consisted of a DC photo-cathode gun; two Wien systems for polarization control [3]; solenoids to set the transverse beam envelope; and several warm radio frequency (RF) and superconducting RF (SRF) cavities. Eighteen 5-cell Cornell-style SRF cavities distributed across two full cryomodules and a quarter cryomodule with two cavities (QCM) set the beam energy. Each full cryomodule (C25) contained eight cavities to produce 25 MeV total energy gain. The warm RF capture cavity ensured the beam energy was matched into the QCM. The remaining warm RF cavities, two bunchers (prebuncher and buncher) and two chopper cavities, along with the capture and QCM set the longitudinal beam properties. The modifications required to upgrade the injector from the 67 MeV design (during the 6 GeV era) to the 123 MeV design (for 12 GeV CEBAF) occurred over several scheduled accelerator down periods, with the major goals and layout changes established beforehand and supported by simulation studies [4, 5].

The first major installation change increased the full energy capability to 123 MeV [6] replacing the second of the injector's two C25s with an early generation C100-style cryomodule (R100) containing eight 7-cell cavities [7]. The second installation, known as Phase 1, concentrated on the gun to up to the chopper region to make it 200 kV capable to reduce space charge effects and in anticipation of the third installation step, known as Phase 2, when the booster module containing one 2-cell and one 7-cell cavity [8] replaces the capture and QCM. Phase 1 (Fig.1b) included upgraded Wien HV capabilities [9], new quadrupoles bracketing each Wien system to address focusing effects, and new solenoids with improved field linearity over a larger aperture [10]. To simplify set up, the prebuncher, a pillbox-style bunching cavity, shifted downstream of the Wien system. The third installation period for Phase 2 (Fig. 1c) in progress now in 2023 focuses on the beamline after the choppers through the exit of the QCM. Phase 2 also continues the solenoid upgrade from Phase 1 and shifts the buncher, a reentrant-style cavity, due to a combination of the prebuncher move, the capture removal, and mechanical design considerations.

CEBAF INJECTOR MODELS

Modeling Note

The injector starts at the gun and ends at the exit of the injection chicane at the entrance of the North Linac. Beam dynamics modeling for the injector uses two tools: GPT [11–13] and elegant [14]. There is overlap between the models, but their purposes are different. The GPT model starts at the gun and extends to the entrance of the two-cryomodule linac section in the injector and contains more detailed element models. The GPT model is responsible for the longitudinal and transverse beam dynamics from the gun through the QCM (now, booster) and ensuring the longitudinal beam dynamics are suitable at the entrance of the injector linac section. The elegant model is responsible for managing the transverse beam optics after the QCM (now, booster) and matching into the main machine.

6 GeV CEBAF Injector Model

The 6 GeV injector GPT model is based on a PARMELA [15] model used to prepare for the G0 experiment [16] and an ASTRA [17] model used in an earlier design study for the 123 MeV injector [4]. The 6 GeV model continued as the 12 GeV upgrade injector model until Phase 1 installation since the first major change to the injector increased its linac energy, downstream of the GPT modeled elements.

Two goals of the model were to ensure it used the most up to date element position information and to document the source of each position and dimension. For the majority of elements, we measured relative positioning using a laser distance meter at fixed locations and a suspended plumb bob that we moved along the beamline. For a small subset, due to tight space constraints, we resorted to ruler measurements. Our measurements agreed with historical survey

* This material is based upon work supported by the U.S. Department of Energy, Office of Science, Office of Nuclear Physics under contract DE-AC05-06OR23177.
† hofler@jlab.org

ISBN: 978-3-95450-231-8 ISSN: 2673-5490 doi: 10.18429/JACoW-IPAC2023-WEPL075

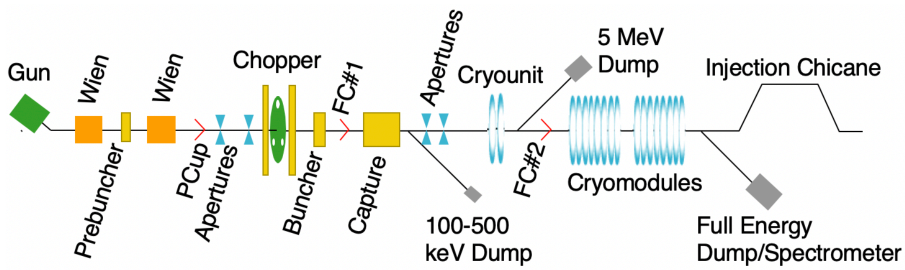

a) The full injector from the gun through the injection chicane merger into the entrance of the North Linac.

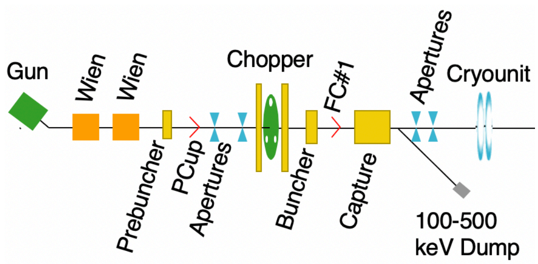

b) The prebuncher is downstream of the Wien systems.

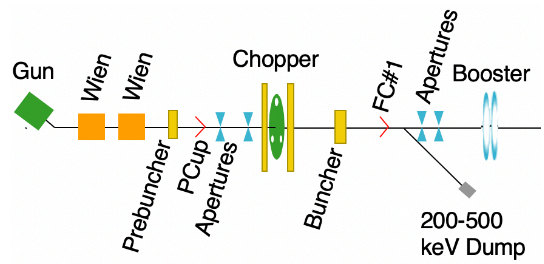

c) Capture removed and new buncher position with the booster.

Figure 1: Injector layouts, not to scale, for (a) the full injector prior to changes for Phase 1 and 2 and the front end for Phases (b) 1 and (c) 2. Magnet elements are not shown. PCup, FC#1, and FC#2 are insertable Faraday cups.

data transmittals from Jefferson Lab's Survey and Alignment group. Any discrepancies were due to documented changes in the beamline subsequent to the official measurements. For positions of internal elements, such as cavities inside cryomodules, we relied on official machine drawings. We recorded position information sources in the GPT files.

Additional goals were to use element setpoints from the accelerator control system and to model elements with field maps from electromagnetic field solvers. The field maps and profiles were organized into folders by element type. For solenoid current setpoints, we scaled the 2D and 3D field maps relative to the current in the coils for a given model. To use gun HV and the gradient setpoint (V/m) for the SRF cavities, we scaled the 1D gun field profile and 3D SRF cavity field maps relative to the integral of the on-axis E_z field. For the prebuncher, buncher, and capture, we regenerated the field maps from the Fourier coefficients used to characterize these fields in the original PARMELA deck and followed the ASTRA convention of scaling the field map by peak amplitude. The chopper cavities and Wien systems were treated as drifts.

A final goal for the model was for it to be flexible enough to perform different types of simulations using the same input file without modification. Having one file (or a set of files that run together as one model) builds confidence in the model and ensures that the same beamline layout, field maps, particle distribution configurations, and position information are used consistently throughout a suite of simulations. Flexibility examples from the 6 GeV model include the ability to run single or multiple particle simulations, perform cavity phasing studies, and run optimizations to find machine settings to provide optimal beam characteristics and performance. This flexibility goal continues to drive improvements in the model for each generation of layout.

One technique for checking that the machine configuration of beam position monitors (BPMs), small steering dipoles (correctors), and solenoid magnets are installed and configured in accordance with established machine conventions is to analyze difference orbit data. With simulations of these measurements, we found the correctors were configured properly and identified two miswired BPMs and three solenoids with incorrect polarity.

Phase 1 Model for 12 GeV CEBAF

During development of the Phase 1 model, we moved the element position information out of the main GPT input file into files dedicated to defined beamline sections. While the overhead in maintaining multiple files is greater, changes are localized to a section during a layout design phase when element positions change often but the relative element order is fixed. The main GPT input file contains the element modeling calls in beamline order since the type of each element is set fairly early in the design phase.

As establishing the suitability of the Phase 1 layout for 200 kV operations was a major goal, we ensured that important optical and RF Phase 1 beamline elements were included in the model. We added the vertical and horizontal Wiens, modeling them with separate overlapping electric and magnetic field maps [18], along with new Wien quads and their field maps. We also upgraded the prebuncher and buncher field maps to 3D versions computed from an electromagnetic field solver. All the solenoids were upgraded to the new design and modeled with field maps. The electrode design is a T-shape (R28-2) [19]. Configuration switches provide easy access to different gun electrode field map models.

ISBN: 978-3-95450-231-8 ISSN: 2673-5490 doi: 10.18429/JACoW-IPAC2023-WEPL075

Two flexibility improvements introduced were incorporating GPT string variables [11] in field map calls and using GPT's multi-run tool [11], mr, to manage simulation configuration parameters and element set points [20]. Centralizing the field map path information into GPT string variables simplifies moving between different file systems since the main route to the field map files is changed in one place as opposed to changing it in each individual map call. Also, the field maps can be gathered and stored in a central location and used by multiple running simulations. Using mr to manage simulation parameters provides an easy way to run and document different simulations because the configuration files are straightforward to inspect, modify, and annotate.

We performed prebuncher bunching studies to determine amplifier requirements. For these simulations, we found settings that bring two particles initially separated by 10° in 1497 MHz RF phase together at a focal point downstream of the prebuncher. Optimizations provided machine settings to use during commissioning and set up for production beam running. Lastly, the model successfully simulated high current beam tests in the injector [21] in preparation for the planned K-Long experiment [22].

Phase 2 Model for 12 GeV CEBAF

In preparation for the Phase 2 mechanical design phase, we developed an early version of the model building on the Phase 1 version with the booster replacing the capture and QCM to finalize the position for the buncher cavity. The original plan from 2011 was for the buncher to remain in its 6 GeV injector location. A subsequent study showed the midway point between the chopper system and the booster was preferable. In this third and final study, factoring in mechanical and installation considerations, we considered three candidate positions, all closer to the booster than the 6 GeV position: closer to the chopper system, the midway point, and closer to the booster. This last study showed that closer to the booster provided the best performance and placed the lowest demands on the prebuncher and buncher. Closer to the chopper system was less optimal but comparable, and it was better than the midpoint position. Since the position closer to the chopper system was best from a mechanical design standpoint while providing comparable beam performance, we chose that position.

The final version of the Phase 2 model implements all the Phase 2 beamline modifications: solenoids with the new design; capture and QCM replaced with the booster; and relocated buncher. Phase 2 uses a new gun cathode geometry, a spherical cathode with a triple-junction point shed (R30-3) [23], and the model provides access to the R30-3 field map while maintaining access to the R28-2 version. The chopper RF cavities are included and modeled with GPT's TMrectcavity elements [11].

The model has been used to determine optimal settings for physics running and buncher amplifier requirements following the bunching method from Phase 1. Planning for K-Long continues with the Phase 2 model [24].

PHASE 1 COMMISSIONING SUMMARY

Commissioning for Phase 1 went smoothly and resulted in successfully establishing physics quality beam for the nuclear physics beam delivery program. We continued to operate the gun at 130 kV without issue. The new solenoid design and separating the prebuncher and Wien systems worked well. Except for some advance studies with beam at 200 keV, we completed our commissioning plan.

Prior to Phase 1, we learned injector reproducibility suffered from beam induced charging on an insertable fluorescent screen beam diagnostic (viewer) early in the injector (< 2 m from the gun). For Phase 1, a small flat metal disc was added to the end of each viewer frame to minimize charge up on the ceramic screen. This change greatly improved the reproducibility and stability of the early injector beam orbit, and the viewer modifications continue in Phase 2. An indication of the modification's success is that charging events were eliminated in the Phase 1 beamline (~ 7 m in length) until the removal of the metal disc from a viewer, ~ 6 m from the gun, due to physical interference with a co-located device. Since the disc's removal, we have had charging events only at that location. For Phase 2, the two devices will be reinstalled at the same location with sufficient clearance to permit restoring the disc to the viewer.

CONCLUSION

We have concurrently maintained and developed improved GPT models for each set of changes in the CEBAF injector layout. The models have been useful for finding new set ups, analyzing data from the operational machine, confirming the viability of new injector layouts and upgrades, and predicting the ability and performance of the injector to support future challenging beam requirements.

We successfully commissioned the Phase 1 injector, and the design worked as expected delivering physics quality beam since the installation and commissioning period. We are preparing to commission Phase 2 in the summer of 2023 and anticipate another successful commissioning experience with continued high quality beam delivery.

ACKNOWLEDGMENTS

Many individuals presently and formerly associated with Jefferson Lab have provided field maps, answered questions, and shared advice on modeling during the development of these GPT models. An incomplete list includes: K. Beard, J. Benesch, F. Hannon, G.A. Krafft, F. Marhauser, G. Palacios-Serrano, M. Tiefenback, H. Wang, S. Wang, B. Yunn, and Y. Zhang. We are very grateful for their assistance. We also appreciate Pulsar Physics for adding new syntax features to GPT.

REFERENCES

[1] R. Abbott, *et al.*, "Design, commissioning and operation of the upgraded CEBAF injector," in *Proc. LINAC'94*, Tsukuba, Japan, Aug. 1994, paper TH-30, pp. 777-779.

ISBN: 978-3-95450-231-8 ISSN: 2673-5490 doi: 10.18429/JACoW-IPAC2023-WEPL075

[2] P. A. Adderley *et al.*, "An overview of how parity-violating electron scattering experiments are performed at CEBAF," *Nucl. Instrum. Methods Phys. Res. Sect. A*, vol. 1046, p. 167710, Jan. 2023. doi:10.1016/j.nima.2022.167710

[3] J. M. Grames *et al.*, "Two Wien filter spin flipper," in *Proc. PAC'11*, New York, NY, USA, Mar.-Apr. 2011, paper TUP025, pp. 862–864.

[4] F. E. Hannon, A. Hofler, and R. Kazimi, "Optimizing the CEBAF injector for beam for beam operation with a higher voltage electron gun," in *Proc. PAC'11*, New York, NY, USA, Mar.-Apr. 2011, paper WEP288, pp. 2023–2025.

[5] R. Kazimi, A. Freyberger, F.E. Hannon, A. S. Hofler, and A. Hutton, "Upgrading the CEBAF injector with a new booster, higher voltage gun, and higher final energy," in *Proc. IPAC'12*, New Orleans, LA, USA, May 2012, paper TUPPR055, pp. 1945–1947.

[6] Y. W. Wang, A. S. Hofler, and R. Kazimi, "Commissioning of the 123 MeV injector for 12 GeV CEBAF," in *Proc. IPAC'15*, Richmond, VA, USA, May 2015, pp. 1920–1922. doi:10.18429/JACoW-IPAC2015-TUPMA037

[7] F. Marhauser *et al.*, "Results of cavity series fabrication at Jefferson Laboratory for the cryomodule R100," in *Proc. IPAC'11*, San Sebastián, Spain, Sep. 2011, paper MOPC113, pp. 340–342.

[8] H. Wang *et al.*, "RF design optimization for new injector cryounit at CEBAF," in *Proc. IPAC'13*, Shanghai, China, May 2013, paper WEPWO073, pp. 2471–2473.

[9] G. Palacios-Serrano *et al.*, "High voltage design and evaluation of Wien filters for the CEBAF 200 keV injector upgrade," in *Proc. IPAC'21*, Campinas, Brazil, May 2021, pp. 1000–1003. doi:10.18429/JACoW-IPAC2021-MOPAB324

[10] J. Benesch, "Injector solenoids: next-to-next-to-final-designs," Thomas Jefferson National Accelerator Facility, Newport News, VA, USA, Rep. JLAB-TN-19-010, Jan. 2019.

[11] Pulsar Physics, General Particle Tracer, http://www.pulsar.nl/gpt.

[12] G. Pöplau, U. van Rienen, B. van der Geer, and M. de Loos, "Multigrid algorithms for the fast calculation of space-charge effects in accelerator design," *IEEE Trans. Magn.*, vol. 40, no. 2, pp. 714-717, Mar. 2004. doi:10.1109/TMAG.2004.825415

[13] S. B. van der Geer, O. J. Luiten, M. J. de Loos, G. Pöplau, and U. van Rienen, "3D space-charge model for GPT simulations of high brightness electron bunches," in *Proc. 7th Int. Conf. on Computational Accelerator Physics (ICAP'02)*, East Lansing, MI, USA, Oct. 2002, M. Berz and K. Makino, Eds., published in *Inst. Phys. Conf. Ser.*, vol. 175, p. 101, 2005.

[14] M. Borland, "elegant: a flexible SDDS-compliant code for accelerator simulation," Advanced Photon Source, Argonne National Lab., Lemont, IL, USA, Rep. LS-287, Sep. 2000.

[15] L. Young and J. Billen, "The particle tracking code PARMELA," in *Proc. PAC'03*, Portland, Oregon, USA, May 2003, paper FPAG029, pp. 3521–3523.

[16] Y. Zhang *et al.*, "A PARMELA model of the CEBAF injector valid over a wide range of parameters," in *Proc. EPAC'04*, Lucerne, Switzerland, Jul. 2004, paper TUPLT165, pp. 1515–1517.

[17] K. Floettmann, ASTRA – A Space charge Tracking Algorithm, https://www.desy.de/~mpyflo/.

[18] J. Benesch, "Modeling the SLAC/JLab Wien filter," Thomas Jefferson National Accelerator Facility, Newport News, VA, USA, Rep. JLAB-TN-15-032, Sep. 2015.

[19] P. A. Adderley *et al.*, "Load-locked dc high voltage GaAs photogun with an inverted-geometry ceramic insulator," *Phys. Rev. Spec. Top. Accel. Beams*, vol. 13, p. 010101, Jan. 2010. doi:10.1103/PhysRevSTAB.13.010101

[20] F. Hannon, private communication, 2017.

[21] S. Pokharel *et al.*, "Bunch length measurement at the CEBAF injector at 130 kV," in *Proc. NA-PAC'22*, Albuquerque, NM, USA Aug. 2022, pp. 917–920. doi:10.18429/JACoW-NAPAC2022-FRXD6

[22] KLF Collaboration, "Strange hadron spectroscopy with secondary KL beam in hall D," *arXiv preprint*, arXiv:2008.08215v3, Mar. 2021. doi:10.48550/arXiv.2008.08215

[23] C. Hernandez-Garcia *et al.*, "Compact -300kV dc inverted insulator photogun with biased anode and alkali-antimonide photocathode," *Phys. Rev. Accel. Beams*, vol. 22, p. 113401, Nov. 2019. doi:10.1103/PhysRevAccelBeams.22.113401

[24] S. Pokharel *et al.*, "CEBAF injector model for K-Long bunch charge at 200 kV," presented at IPAC'23, Venice, Italy, May 2023, paper WEPL054, this conference.